POLITECNICO DI TORINO
Repository ISTITUZIONALE

Self-standing gelatin- methacryloyl 3D structure using Carbopol-embedded printing

Original
Self-standing gelatin- methacryloyl 3D structure using Carbopol-embedded printing / Villata, S., Frascella, F., Gaglio, C.G., Nastasi, G., Petretta, M., Pirri, C., Baruffaldi, D.. - In: JOURNAL OF POLYMER SCIENCE. - ISSN 2642-4169. - ELETTRONICO. - 62:11(2024), pp. 2259-2269. [10.1002/pol.20240037]

Availability:
This version is available at: 11583/2991605 since: 2024-09-10T09:48:19Z

Publisher:
Wiley

Published
DOI:10.1002/pol.20240037

Terms of use:

This article is made available under terms and conditions as specified in the corresponding bibliographic description in the repository

Publisher copyright
Wiley postprint/Author's Accepted Manuscript

This is the peer reviewed version of the above quoted article, which has been published in final form at http://dx.doi.org/10.1002/pol.20240037.This article may be used for non-commercial purposes in accordance with Wiley Terms and Conditions for Use of Self-Archived Versions.

(Article begins on next page)

18 November 2026

Physiology International
DOI: 10.1556/2060.2026.00745

Effects of resistance on spatiotemporal variables and electromyographic activity of the hamstrings during maximal sprint acceleration

DÁNIEL CSALA[1*], TAIAN MARTINS VIEIRA[2,3], JÁNOS TÓTH JR.[4], ÖRS SEBESTYÉN[1], JÓZSEF TIHANYI[1] and ANDRÁS HEGYI[1]

[1] Department of Kinesiology, Hungarian University of Sports Science, Budapest, Hungary

[2] Laboratory for Engineering of the Neuromuscular System, Department of Electronics and Telecommunications, Politecnico di Torino, Turin, Italy

[3] PolitoBIOMed Lab—Biomedical Engineering Lab and Department of Electronics and Telecommunications, Politecnico di Torino, Torino, Italy

[4] Department of Football, Hungarian University of Sports Science, Budapest, Hungary

Received: September 10, 2025 • Revised manuscript received: March 10, 2026 • Accepted: March 16, 2026

© 2026 The Author(s)

ABSTRACT

This study aimed to examine how horizontal resistance affects spatiotemporal kinematics and the electromyographic (EMG) activity of the biceps femoris long head (BFlh) and semitendinosus (ST) in sprinting.

Eleven trained male football players ($n = 10$) performed 40 m sprints under three resistance conditions (0, 10, and 20% decrements in maximum sprint velocity, %vdec). Spatiotemporal variables were captured using a photoelectric system, while high-density surface EMG recorded regional muscle activity in BFlh and ST. Analyses were conducted at both maximum speed and matched running speed across conditions to isolate the effects of resistance and velocity. Regional EMG distribution (centroid analysis) was evaluated in a subset of participants with sufficient signal quality ($n = 5$).

At matched speed, spatiotemporal variables showed no differences across resistance levels, however ST EMG activity was higher at 0 $\%v_{dec}$ condition compare to 10 $\%v_{dec}$ condition during the swing phase (70.50–75.70% $P = 0.001$). At maximum speed, moderate differences were found in step length and

* Corresponding author. Alkotás utca 42-48., 1123 Budapest, Hungary. Tel.: +36202928847. E-mail: daniel.csalahk@gmail.com

Unauthenticated | Downloaded 05/06/26 10:44 AM UTC

frequency. ST EMG activity was higher at 0 $\%v_{dec}$ compare to 20 $\%v_{dec}$ during stance phase (10.22–18.02% $P = 0.001$) and 0 $\%v_{dec}$ compare to 10 $\%v_{dec}$ during swing phase (68.50–71.00% $P = 0.004$). Centroid analysis revealed individual-specific shifts in the region of the highest EMG amplitude within the muscles.

Moderate horizontal resistance has no or small impact on global hamstring EMG activity or sprint mechanics at matched speed but may induce individual shifts in regional EMG activity. Future studies should examine how these acute neuromuscular responses translate into long-term neuromuscular adaptations.

KEYWORDS

hamstring, HD-sEMG, football, resisted sprint, regional activity

INTRODUCTION

The skill of sprinting holds significance across various sports like soccer, football, rugby, and athletics [1, 2]. High propulsive forces applied to the ground predict acceleration performance and contribute to maintaining high running speed [3, 4]. Modelling studies [5, 6] have shown the vital role of hamstrings in sprinting by contributing significantly to horizontal propulsion, especially at high running speed. Morin et al. [7] have shown that the amount of horizontal ground reaction force produced during sprint acceleration is related to the excitation of the biceps femoris long head (BFlh) prior to ground contact. Hence, BFlh might serve to pre-activate the muscle and prepare for an effective propulsion in the stance phase. Additional to the BFlh, the semitendinosus (ST) is likely to contribute to superior sprint performance [8, 9] by generating large hip extension torques [10] at maximal velocity phase.

Running speed significantly alters running kinematics and kinetics, requiring adaptive changes in joint motion and muscle function. For instance, at slower speeds runners increase speed primarily through longer step length, whereas at faster speeds they rely more on higher step frequency [11]. Joint ranges of motion and angular velocities—especially at the hip and knee—also increase with increasing running speed. In the stance phase, the ankle plantar flexors dominate energy generation at low speeds but are overtaken by hip extensors at higher speeds. Meanwhile, the hamstrings perform negative work during the swing phase, which also increases with increasing speed [11].

Previous studies found substantial increase in hamstring electromyographic (EMG) activity with increasing running speed [12–14]. However, these studies examined hamstrings EMG activity at steady-speed running, and there are only a few studies that examined hamstrings EMG activity in a maximal overground sprint acceleration. During overground sprinting, the EMG activity of hamstring muscles is relatively high from the terminal swing to the early stance phase [15], and increases with increasing running speed [16]. Consistent with these findings, recent evidence confirmed that hamstring EMG activity—especially in the BFlh—increases substantially with speed, showing a 23% rise at maximum velocity [17].

Resisted sprinting is a common training method to improve sprint acceleration performance [18, 19]. Resistance is often applied by using sleds, resistance bands, resistance chute or motorised equipment to enhance muscular strength and power during sprinting. A number of studies have assessed the acute effects on kinematics in response to increasing resistance. They found a

Unauthenticated | Downloaded 05/06/26 10:44 AM UTC

decreased step length, decreased swing phase duration and step frequency, but increased contact time [20, 21], when increasing the resistance by 10–40 % body mass, relative to unresisted sprinting. Furthermore, resistance increased trunk lean [19] and decreased knee flexion angle [22] in the acceleration phase. In line with these kinematic adaptations, recent findings [17] demonstrated that increasing resistance during sprinting leads to a systematic reduction in hamstring muscle activation, particularly in the stance phase. The effects of resistance were substantial in the semitendinosus and semimembranosus, but not as much in the biceps femoris long head. However, these studies only recorded from a small muscle region when examining the interplay between hamstring muscles, without considering possible proximal-distal differences in EMG activity. Another limitation of these studies is that the effect of resistance was compared at maximum speed of each resistance condition. However, the higher the resistance the lower the maximum running speed, i.e., it is challenging to understand whether the effects are due to increasing resistance or decreasing the speed at which these conditions are compared. To better understand the acute effects of increasing resistance, it has been suggested to compare speed-matched steps at different resistance conditions [23].

The aim of the current study was to examine the impact of increasing resistance in sprinting on the spatiotemporal characteristics of the sprint and on the EMG activity of the BFlh and ST. We aimed to perform the analysis at the maximum speed of each condition (i.e., matched sprint phases but different speed), and at matched speed (i.e., different sprint phases) to separate the effect of running speed and resistance. We hypothesized that, when comparing each resistance condition at its maximum speed, regional activation of the BFlh will shift proximally and the EMG amplitude will increase with higher maximum speeds, whereas semitendinosus (ST) activity will remain relatively stable. This is suggested by Cerone et al., who found proximal shifts in BFlh EMG centroid with increasing running velocity [24]. If running velocity is the primary determinant of regional hamstring excitation, then when steps are matched for running speed across resistance conditions there will be no systematic differences in regional EMG distribution or overall EMG amplitude for BFlh and ST. Alternatively, if external load imposes an additive effect independent of velocity, increasing resistance will produce increased EMG amplitude and alterations in the regional distribution of activation (for BFlh and/or ST) regardless of whether runs are compared at matched speed or at each condition's maximum speed.

METHODS

Participants were 11 male amateur football (soccer) players (age 22.7 ± 2.8 years, height 1.81 ± 0.04 m, weight 78.5 ± 6.8 kg) with regular training and match exposure (minimum three times per week), and were recruited from different local teams between 2022 October and 2024 Jun. Participants had no known history of hamstring injury or any lower extremity/lower back injuries in the past. The players who participated in the study did not have prior experience with the resisted sprint modalities employed. The final sample size was limited due to injuries and data quality issues inherent to high-density EMG recordings during maximal sprinting. The planned sample size was informed by previous studies [14, 23] investigating sprint kinematics and region-specific hamstring EMG activity using similar methodologies with fewer than 15 participants. All participants provided written informed consent for this study, which was approved

Unauthenticated | Downloaded 05/06/26 10:44 AM UTC

(TE-KEB/34/2020) by the ethics committee of Hungarian University of Sports Science. Testing procedures were performed in accordance with the Declaration of Helsinki.

Procedures

Before the main testing session, two familiarisation sessions were implemented where the participants became familiar with the tools, procedures, and expectations. The familiarization sessions began with general warm up, which consisted of running at gradually increasing intensity (from 60 to 100% intensity) of 5 × 40 m sprints series and dynamic stretching. During the familiarisation, participants performed two 40 m sprints at three different resistance conditions to determine the required resistance for the targeted decrements of individual maximum velocity (%v_{dec}). The familiarization always started with the free sprint (0 %v_{dec}), followed by the targeted 10 %v_{dec} and 20 %v_{dec} resistance conditions. The free sprint meant a minimal resistance was applied (0.488 kg) by the robotic resistance device.

Following the familiarisation sessions, the measurement session began with preparation, then the above warm-up protocol was followed by two free sprints. The individual maximum velocity of the measurement session was used to calculate the 10 and 20 %v_{dec} target for the testing (maximal speed – maximal speed x target %v_{dec}). The participants performed the 40 m sprints at each resistance condition in a randomized order. The number of the sprints at each condition varied between one and three repetitions, depending on how many repetitions were needed to find the resistance which resulted in no or minimal deviation from the target decrements of individual maximum velocity (±2.0 %). A minimum of five minutes' rest was provided in-between sprints to ensure recovery was maximised between trials [25]. Each trial required the athlete to take up a standing split-stance behind a marked line, and sprint forward without any backward movement prior to accelerating forward. Verbal encouragement was provided to ensure a maximal effort throughout each trial.

Data collection

Resistance was applied with a robotic resistance device (dynaSpeed, Ergotest Technology AS, Langesund, Norway). The motor was attached to a composite fiber cord that was wrapped around a spool and was attached to the athlete by a hip harness around the pelvis. The device consists of a line connected to a motor that can smoothly adjust pulling force per 0.1 kg. The subject's speed was collected with the dynySpeed device (sampling frequency = 1,000Hz) and recorded with MuscleLab software (v10.202.93.5131, Ergotest Technology AS, Langesund, Norway).

A 40-m long optical measurement system consisting of two parallel bars placed along the running track containing light-emitting diodes (LED) was used to collect spatiotemporal kinematic data of the running at a sampling frequency of 1,000 Hz with an accuracy of 0.01 m (Optojumo, Microgate Inc, Italy). The system detects an interruption in communication between the transmitter and receiver bars and uses the duration of the interruption to calculate kinematic variables such as step velocity, step length, step frequency, contact time, and flight time. Previous study reported that calculations of step parameters during running show high concurrent validity with force plates (mean bias = 0.4–2.7 %, intraclass correlation coefficient = 0.96–0.99) [26].

Unauthenticated | Downloaded 05/06/26 10:44 AM UTC

Monopolar EMG data was collected with a 64-channel high density surface EMG (HD-sEMG, Sessantaquattro, Bioelettronica, Turin, Italy). Signals were amplified (256 V/V) and then digitized at 2,000 Hz with a 16 bit A/D converter (BioLab + v1, OT Bioelectronica). Ultrasonography (Hitachi-Aloka EUB 405 plus, Japan) was used to identify and mark the borders of the right BFlh and ST: a linear array of 16 electrodes (10 mm inter-electrode distance; OT Bioelectronica, Torino, Italy) was placed along each muscle, after shaving and cleaning the skin. A muscle-specific electrode placement was then applied. For the BFlh, channels 8–9 from the distal end were aligned with the midpoint between the ischial tuberosity and the popliteal fossa, ensuring that the midpoint of the electrodes corresponds accurately to recommended anatomical landmarks [27]. In the case of the ST, the array was positioned one centimeter distal to the tendinous inscription of the muscle [28, 29]. It is important to note that this placement focuses on the distal portion of the muscle belly, which may limit the representation of the proximal compartment that has been shown to have distinct innervation patterns. In both cases the electrode medio-lateral placement was the midway of the muscles' borders determined by ultrasonography and it was aligned parallel to the muscle longitudinal axis (Fig. 1). The arrays were secured to the skin using double-sided adhesive pads, and 20 µl of conductive gel was applied into each electrode cavity to ensure proper skin-electrode contact. A reference electrode was placed over the sacrum. Synchronisation between the HD-sEMG and Optojump systems

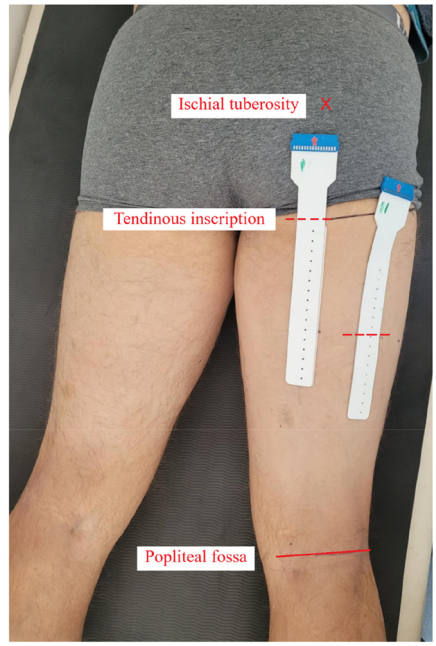


Fig. 1. Linear EMG arrays were placed over the biceps femoris long head (BFlh) and semitendinosus (ST) after defining muscle borders with ultrasonography
For the BFlh, the middle of the EMG arrays were aligned with the midpoint between the ischial tuberosity and the popliteal fossa. For the ST, the array was positioned one centimeter distal to the tendinous inscription of the muscle

Unauthenticated | Downloaded 05/06/26 10:44 AM UTC

was ensured by tapping a force sensor (FlexiForce™ Standard Model A201) before each sprint that was taped onto the ground between the Optpjump bars. The force signal was sampled synchronously with the EMG signals; thereby, the event of tapping was detected by both the Optojump and HD-sEMG systems simultaneously. The force sensor was connected to the HD-sEMG system by a cable for the synchronisation procedure, which was then removed for the sprint.

Data analysis

To examine the differences between resistance conditions in the spatiotemporal and HD-sEMG variables, two different approaches were implemented: sprint phase-matched and speed-matched. For the sprint phase-matched approach, the three fastest steps in each resistance condition were averaged and compared between conditions. The fastest steps were defined based on step speed calculated by Optojump Next software after ensuring that no steps in the deceleration phase were included in the analysis using the acceleration data extracted from the Dynaspeed, which estimated the horizontal velocity of the body centre of mass. This method allows for comparisons at the same phase of the sprint (i.e., maximum speed). However, in this case the absolute speed is different between conditions due to the different resistance applied in each condition. Therefore, for speed-matched comparisons, we also compared conditions after selecting matched speed steps: three steps in the free sprint and three steps in the 10 $\%v_{dec}$ were matched to the fastest steps in the 20 $\%v_{dec}$ condition. For this, we selected consecutive steps, the average of which resulted in a similar speed to the average speed of the fastest steps in 20 $\%v_{dec}$. As a result, the speed in the matched condition was $6.67 \pm 0.59\ m{\cdot}s^{-1}$ for 0 $\%v_{dec}$, $6.60 \pm 0.43\ m{\cdot}s^{-1}$ for 10 $\%v_{dec}$, and $6.64 \pm 0.52\ m{\cdot}s^{-1}$ for 20 $\%v_{dec}$.

Spatiotemporal variables such as step length, step frequency, contact time, and flight time were extracted from the *Optojump next* software. The contact time was considered to begin once at least one LED was activated and finished once the number of activated LEDs returned to 0. The minimum threshold for flight time and contact time was set at 0.01 s. Data were imported to Matlab (MathWorks, Natick, MA, USA) to be processed along with the EMG data.

EMG data and the trigger signal from the force sensor were imported to Matlab. First, the EMG data was time-aligned with the Optojump data by removing all signals before the rise of the force signal detected by the force sensor. Then, the processing of EMG signals started with a thorough visual inspection of the monopolar and bipolar signals. During the visual inspection EMG signals were filtered offline using a 2^{nd} order zero-lag Butterworth band-pass filter (15–350 Hz) and 50 Hz notch filter was applied. Monopolar channels of insufficient quality were excluded from the analysis [30]. For the BFlh and ST, a total of 11 ± 5 and 11.5 ± 4 (median ± interquartile range) channels were analysed, respectively. Bipolar EMGs were derived from the raw monopolar signals then bipolar signals were filtered offline using a 4th order zero-lag Butterworth band-pass filter (10–500 Hz) and subsequently rectified. A 20 Hz low-pass, zero-phase Butterworth filter was then applied to each channel to smooth the signals for curve analysis. Smoothed curves of all channels were averaged to estimate the overall excitation of each muscle separately. Foot strike (FS) and toe-off (TO) events were defined based on Optojump spatiotemporal kinematic data. Then, EMG curves for each muscle were time-normalised for each stride (1–101 points from FS until the consecutive FS) and then averaged for each resistance condition and individual. These curves were included in the statistical analysis. Regional

Unauthenticated | Downloaded 05/06/26 10:44 AM UTC

differences in muscle excitation under resisted conditions were evaluated by calculating the centroid of channels, including channels with EMG envelopes exceeding 70% of peak amplitudes [31]. This analysis was performed on a small number of subjects ($n = 5$) who had at least nine high-quality channels evenly distributed across the muscle. The number of segmented channels was used to estimate the size of the activated muscle region, while the centroid was used to identify the central location of this activated region within the muscle.

Statistical analysis

Statistical analysis on the kinematic variables was performed using IBM SPSS Statistics (IBM SPSS Statistics for Windows, Version 30.0, IBM Corp. New York). A Shapiro–Wilk test was used to test for normal distribution and Levene test for homogeneity of variance. Two-way ANOVA with repeated measures was used to test for differences between resistance conditions and two different calculation approach in the case of normal distribution (Step velocity, Step length, Step frequency, Flight Time). A Related-Samples Friedman's Two-Way Analysis test was performed in the case of non-normally distributed kinematic variables (Contact Time). The significance level was set to 0.05, and in case of a significant main effect, post hoc tests were applied with Bonferroni corrections.

EMG curve analyses were conducted using Statistical Parametric Mapping (SPM, v0.4, www.spm1d.org) in Matlab. Two-way repeated measures ANOVAs were performed across time-normalized running strides for each muscle. SPM{F}test statistics were calculated to test resistance condition x EMG interactions for each muscle. Family-wise type I error rate was set at 0.05. In case of an interaction at any timepoint across the conditions and speeds, locations of the differences were tested using paired-sample t-tests with Bonferroni correction ($P = 0.017$). In all SPM analyses, the test statistic (SPM{F} or SPM{t}) was calculated first, and the critical threshold (F^* or t^*) was then defined. Whenever the test statistic trajectory crossed the critical threshold (forming so-called suprathreshold clusters) the difference was considered statistically significant. Finally, P values were calculated for each suprathreshold cluster. SPM technical details are described elsewhere [32, 33].

RESULTS

Spatiotemporal kinematics

The averaged step velocity at maximal speed under 0, 10 and 20 $\%v_{dec}$ resistance conditions were 8.03 ± 0.51, 7.30 ± 0.46 and 6.73 ± 0.45 $m{\cdot}s^{-1}$, respectively. In the case of the matched speed the average step velocity was 6.78 ± 0.48, 6.67 ± 0.37 and 6.73 ± 0.45 $m{\cdot}s^{-1}$, respectively. Significant condition x speed interaction effect was found (Fig. 2). At maximal speed, step velocity was significantly higher ($P < 0.001$) at 0 $\%v_{dec}$ condition compared to 20 $\%v_{dec}$ condition (+16% $CI_{95\ \%}$ [11.6 %, 20.7 %]). However, no significant differences were found between conditions at matched speed ($F [2, 27] = 5.149$, $P = 0.863$, $\eta 2 = 0.011$). Step velocity was significantly higher at maximal speed compared to matched speed in both the 0 $\%v_{dec}$ ($t = 10.526$, $P < 0.001$, $d = 0.374$) and 10 $\%v_{dec}$ ($t = 7.086$, $P < 0.001$, $d = 0.281$) conditions (16 % $CI_{95\ \%}$ [12.2 %, 18.9 %] and 9 % $CI_{95\ \%}$ [5.9 %, 11.4 %], respectively).

Unauthenticated | Downloaded 05/06/26 10:44 AM UTC

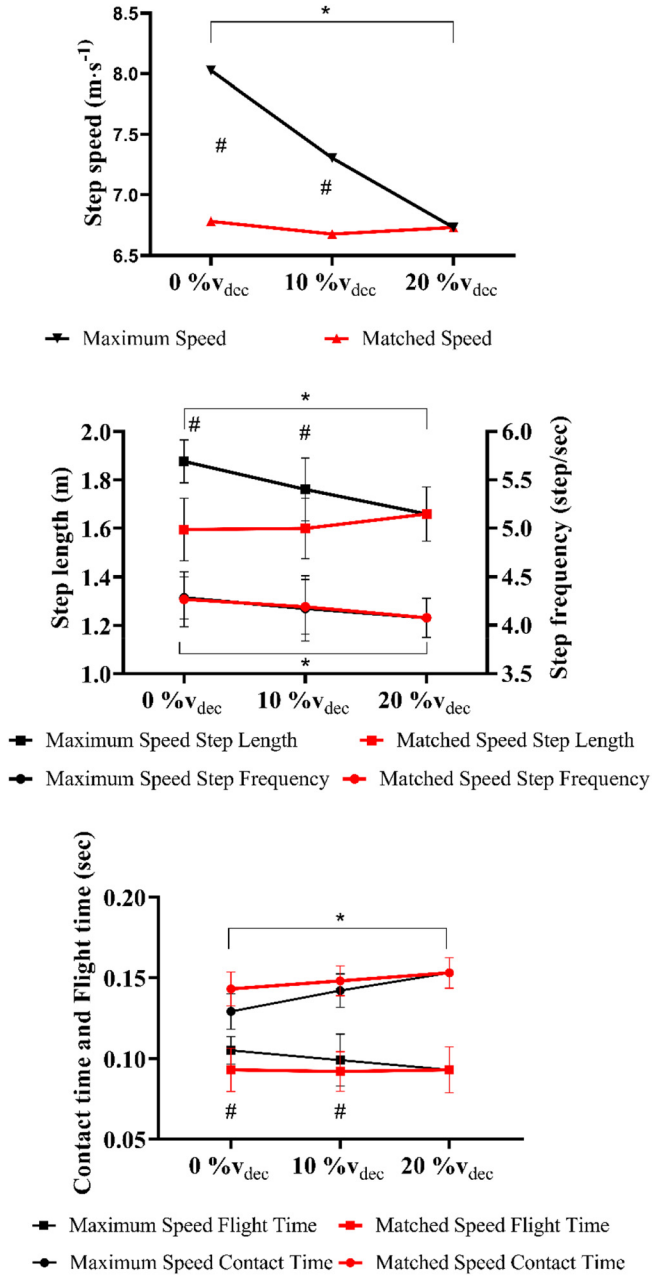


Fig. 2. Spatiotemporal variables between resistance conditions
Red lines represent matched speed steps, black lines represent maximal speed steps. Differences between resistance conditions represented by asterisks (*) in same color as the represented lines. Differences between speeds at a given resistance condition represented with hash symbols (#)

Unauthenticated | Downloaded 05/06/26 10:44 AM UTC

In the case of step frequency, we found significant main effect of resistance condition only (Fig. 2). Post-hoc comparison showed higher ($P = 0.002$) step frequency at the 0 $\%v_{dec}$ compare to 20 $\%v_{dec}$ condition at maximal speed (+5 % $CI_{95\ \%}$ [2.0 %, 7.3 %]). Step frequency was not significantly different between the maximal and matched speed at any given conditions (F [1, 9] = 0.001, $P = 0.971$, $\eta 2 = 0.000$).

For step length, significant effects were found in the case of the resistance, speed, and resistance x speed interaction. Post-hoc comparison showed at maximal speed, step length was significantly longer ($P < 0.001$) at 0 $\%v_{dec}$ condition compared to 20 $\%v_{dec}$ condition (+12 % $CI_{95\%}$ [8.4 %, 14.8 %]). No significant differences were found between conditions at matched speed (F [2, 27] = 0.856, $P = 0.436$, $\eta 2 = 0.600$). Step length was significantly longer at maximal speed compared to matched speed both 0 $\%v_{dec}$ ($t = 8.527$, $P < 0.001$, $d = 10.458$) and 10 $\%v_{dec}$ ($t = 9.325$, $P < 0.001$, $d = 5.482$) conditions (15 % $CI_{95\%}$ [11.1 %, 19.0 %] and 9 % $CI_{95\%}$ [7.0 %, 11.4 %] respectively).

In the case of flight time no significant differences were found between conditions neither at maximum speed (F [2, 27] = 1.683, $P = 0.205$, $\eta 2 = 0.111$), nor at matched speed (F [2, 27] = 0.101, $P = 0.904$, $\eta 2 = 0.007$). Flight time was significantly longer at maximal speed compared to matched speed, for both 0$\%v_{dec}$ ($t = 3.744$, $P = 0.005$, $d = 0.011$) and 10$\%v_{dec}$ ($t = 3.774$, $P = 0.004$, $d = 0.006$) conditions (13 % $CI_{95\%}$ [4.8 %, 20.2 %] and 8 % $CI_{95\%}$ [3.0 %, 12.1 %] respectively).

The related-Samples Friedman's Two-Way Analysis test revealed significant shorter contact time at maximal speed at 0 $\%v_{dec}$ compare to 20 $\%v_{dec}$ condition (−18 % $CI_{95\%}$ [−3.9 %, −21.2 %]). No significant differences were found between conditions at matched speed. TContact was not significantly different between the maximal and matched speed at any given conditions (Fig. 2).

EMG results

Figure 3 presents the EMG activity at different resistance conditions. Differences were found in ST EMG activity for a short period during maximal speed steps between 0 $\%v_{dec}$ and 20 $\%v_{dec}$ at stance phase (10.22–18.02% $P = 0.001$) and between 0 $\%v_{dec}$ and 10 $\%v_{dec}$ at swing phase (68.50–71.00% $P = 0.004$). ST EMG activity showed differences in EMG activity during matched speed between 0 $\%v_{dec}$ and 10 $\%v_{dec}$ in the swing phase (70.50–75.70% $P = 0.001$). There was no difference in the BF or ST activity between the maximum and matched speed conditions.

Centroid results

Figure 4A represents a single participant's EMG envelopes from the ST muscle. The location of the greatest EMGs within the ST and BF between resistance conditions are presented on (Fig. 4B). During the stance and the swing phase of running, individual variations were present, with the EMG amplitude centroid shifting by approximately 2–5 cm in either proximal or distal directions.

DISCUSSION

This study aimed to investigate the effects of horizontal resistance on sprint mechanics and electromyographic (EMG) activity in the hamstrings, particularly in the biceps femoris long head (BFlh) and semitendinosus (ST), during maximal sprint acceleration. Our results revealed

Unauthenticated | Downloaded 05/06/26 10:44 AM UTC

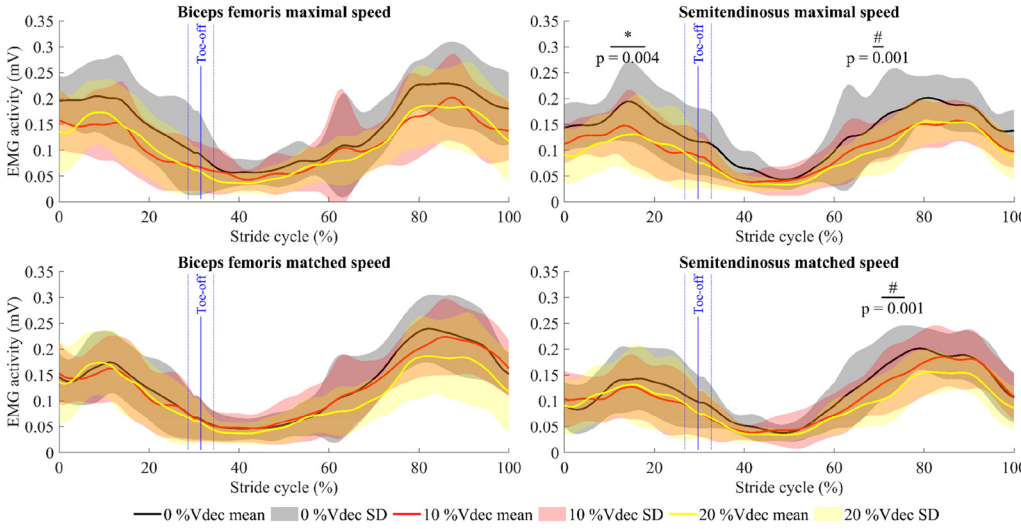


Fig. 3. Stride cycle normalized EMG activity curves (0 % touchdown to 100% next touchdown) Maximal speed for BFlh (top left panel), ST (top right panel) and the matched speed (BFlh and ST are bottom left and bottom right panel respectively. Solid lines represent mean values, whereas the shaded areas the standard deviation. Mean value of the toe-off represented by solid vertical blue lines, dashed vertical lines are the standard deviation of the toe-off between subjects. Comparison between resistance conditions was calculated via spm statistics. Where the curves are significantly different from each other a horizontal black solid line was drawn (* difference between 0 %vdec and 20 %vdec, # difference between 0 %vdec and 10 %vdec)

minimal differences in spatiotemporal and EMG variables between resistance conditions when compared at matched running velocities, supporting the hypothesis that resistance does not substantially alter sprint mechanics at equivalent speeds. Although moderate spatiotemporal differences were observed at maximal running speed, these were not accompanied by notable alterations in BFlh and ST EMG activity. Regarding sprint kinematics, our findings at maximal velocity running align with Osterwald et al. [22], who found decreased step lengths with heavier loads. Additionally, in the previous study, this was accompanied with an increased trunk lean, potentially limiting athletes' ability to transition into optimal sprinting posture during maximal velocity phases. Similarly, van den Tillaar et al. [34] observed decreased step length, increased contact time, and minimal change in step frequency with incremental resistance, particularly within the acceleration phases (first 10–20 m) of resisted sprinting. However, our results demonstrated minor alterations in sprint kinematics when velocity was matched across different resisted conditions, reinforcing previous findings that external resistance does not impact sprint mechanics substantially at matched running speeds [23]. Collectively, these observations emphasize that the critical determinant of kinetic and kinematic variables during sprint acceleration is the running velocity itself, rather than the imposed horizontal resistance.

We found relatively consistent EMG activity across resistance levels from light to medium. It has been shown that relatively heavier resistance produces significant changes in muscle excitation when compared at the maximum speed of each condition [17, 35]. For example, Macchi

Unauthenticated | Downloaded 05/06/26 10:44 AM UTC

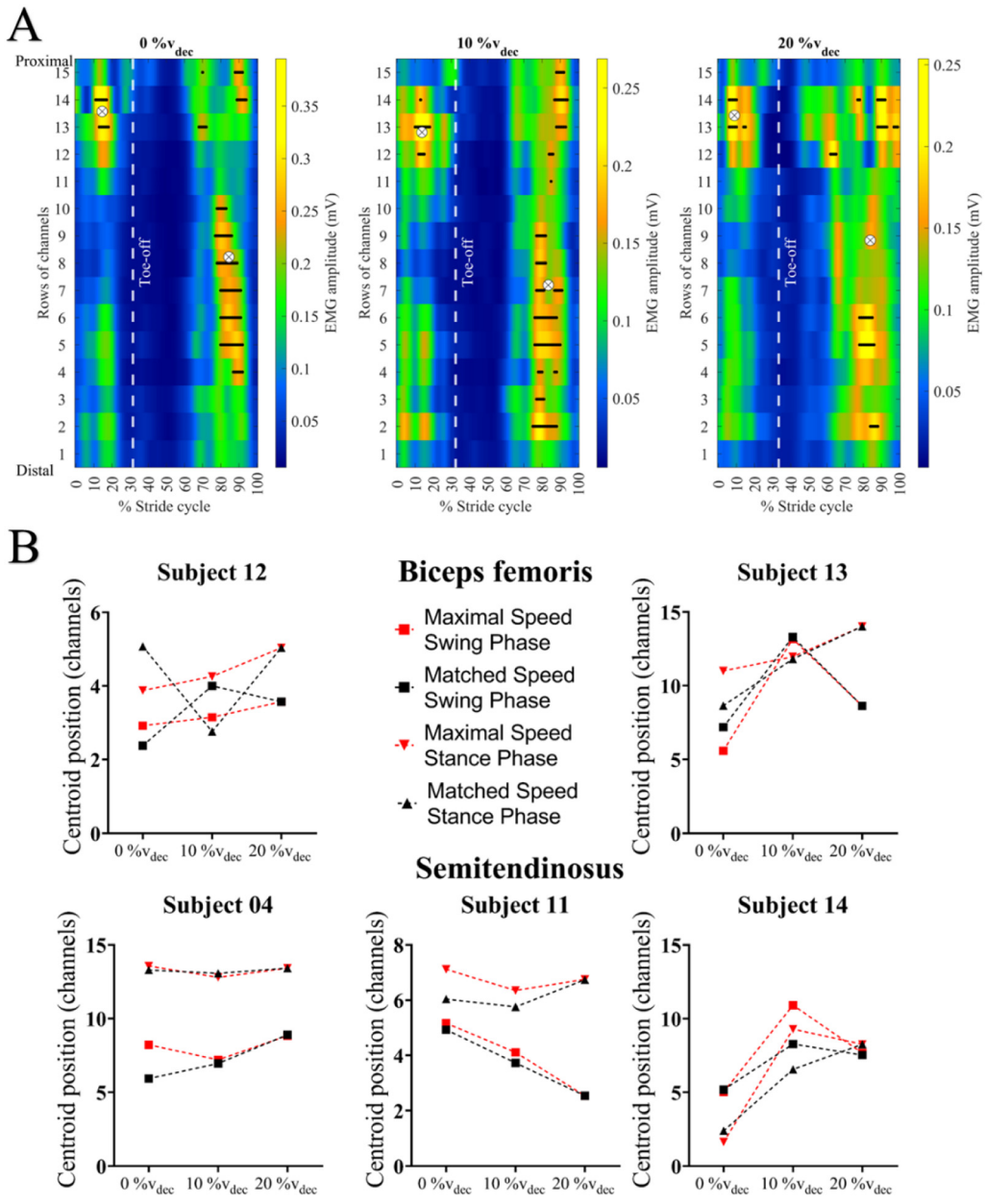


Fig. 4. (A) Spatio-temporal representation of EMG envelopes from the ST muscle (1–15 channels, distal to proximal respectively), for a single participant and for the 0 %vdec (left) 10 %vdec (middle) and 20 %vdec (right) resistance condition at maximal speed steps. Crossed circles denote the centroids computed for stance phase and swing phase of the stride cycle. Mean value of the toe-off represented by dashed vertical lines, (B) Individual-level centroid results for the different resistance conditions and two muscles in stance and swing phase

Unauthenticated | Downloaded 05/06/26 10:44 AM UTC

et al. [17] used 25 and 75 % of body weight (%BW) resistance and reported decreased EMG activity in the BFlh, ST and SM muscles during the maximal speed phase with increasing resistance. Conversely, van den Tillaar [35] found activity changes in ST only for female sprinters at 30 and 40 % BW resistance. We measured at relative moderate 10 $\%v_{dec}$ (~5.9 ± 0.7 %BW) and 20 $\%v_{dec}$ (~11.8 ± 0.9 %BW) resistance due to their documented effect on the speed at maximal velocity phase in different athletic populations [36, 37]. The incremental resistance used here (up to 20 % decrement in velocity) had no substantial effect on the EMG activity of BFlh and ST in a trained male population when compared at the same sprint phase between conditions. Future research should investigate dose-response relationships between resistance magnitude and hamstring activation to determine the threshold at which significant acute neuromuscular adaptations occur in the hamstrings.

The centroid analysis revealed individual tendencies for regional shifts in both BFlh and ST when different resistances were applied. These shifts were observed at matched as well as at maximum running speeds. This suggests that changes in the intramuscular distribution of EMG activity appears independent of running speed. Cerone et al. [24] demonstrated that increasing running speed elicits a shift in EMG activity toward the proximal region of the BFlh muscle when increasing running speed from 70 to 100% of the maximum running speed. Based on a small number of subjects in our study, we also observed a proximal shift toward the proximal origin of the BFlh with increasing resistance both at stance and swing phase. The observed effects in ST were less consistent across individuals, although our sample size was very limited. Because these activity shifts persist across resistance conditions in the matched speed conditions, it seems that underlying individual activation strategies related to the resistance. This theory is reinforced by Macchi et al. [17], who observed high inter-individual variability in the EMG activity change during the swing phase of maximal velocity resisted sprint running. Furthermore, their analysis confirmed that alterations in hamstring EMG activity were predominantly present around their peak activation periods, i.e., in the first half of stance and the late swing phase. While strong conclusions cannot be drawn, this suggests that future studies should investigate the distribution of EMG activity at an individual level instead of relying on group level analyses. Additionally, the heterogeneity in the EMG amplitudes within the muscle reinforces previous suggestions to use high-density EMG to accurately describe the excitation of hamstring muscles in sprinting [14]. It is worth noting that during dynamic movements, shifts between the muscle and the surface electrodes can affect the accuracy of high density EMG recordings [30]. Therefore, regional differences in activation, especially under non-isometric conditions, should be interpreted with caution due to inherent limitations of surface EMG [38, 39].

Several limitations warrant consideration. First, our study had a limited sample size ($n = 10$), which reduces statistical power and limits generalizability. In addition, the regional EMG (centroid) analysis was conducted in a limited subset of participants ($n = 5$) who met strict signal-quality criteria required for high-density EMG recordings during maximal sprinting. As a result, these centroid findings should be interpreted as exploratory and descriptive, and no group-level inferences can be drawn. Second, a fundamental limitation of surface EMG is the potential contamination of signals by neighbouring muscles' excitation (i.e., cross-talk). Given we analysed single-differential EMGs collected by 1 cm spaced electrodes [38] positioned centrally within the target muscles, we believe that cross-talk from neighbour muscles to be negligible. However, it is important to acknowledge that our electrode placement strategy for the

Unauthenticated | Downloaded 05/06/26 10:44 AM UTC

semitendinosus (ST) muscle focused primarily on its distal compartment, with the array positioned 1 cm distal to the tendinous inscription. While this methodological choice aimed to minimize interference from different innervation sites and enhance the clarity of localized findings, it necessarily limits our representation of the proximal compartment. Third, EMG amplitudes may not reflect the neural input to the muscle, although intramuscular differences have also been observed at the level of the motor units [39]. Fourth, the present study did not include analyses specifically designed to examine the effects of horizontal resistance on the segmental and joint kinetics and kinematics, which should be addressed in future studies to comprehensively understand the link between the neuromuscular and mechanical characteristics of resisted sprints. Finally, participants had no prior experience with the resisted sprint modality employed in this study, which may have influenced sprint mechanics and neuromuscular activation patterns. However, two dedicated familiarization sessions were implemented before testing to minimize learning effects, although residual influences of task novelty cannot be fully excluded. Additionally, the participants in this study were limited to well-trained male amateur football players and it remains possible that the effects of horizontal resistance may vary according to sex, age, running technique, or physical fitness level. These factors should be explored in future investigations.

In conclusion, our findings suggest that light-to-moderate horizontal resistance does not affect sprint spatiotemporal kinematics at matched speeds and does not alter hamstring EMG amplitudes. These insights contribute to a growing body of literature emphasizing the nuanced acute effect of resisted sprinting on sprint kinematics and muscle function. Future studies should examine higher resistance ranges (>50% velocity decrement) and include larger, longitudinal samples to determine dose–response effects and individual variability in intramuscular EMG responses.

Author contributions: D.CS., and Ö.S. conceived and conducted the measurements. J.T. Jr organized the recruitment and project administration. D.CS., A.H., and T.M.V analysed the results and D.CS. and A.H. interpreted them. D.CS. and A.H. drafted the manuscript, and J.T., and A.H. supervised the entire project and provided funding. All authors reviewed the manuscript.

Competing interests: The authors have no competing interest to report.

Ethics approval: All data collection adhered to the principles of the Declaration of Helsinki to ensure player and team confidentiality, with ethical approval obtained from the local university ethics board (approval number: TE-KEB/34/2020).

Data availability statement: The data are available upon reasonable request to the corresponding author. The data are not publicly available due to privacy reasons.

Consent to publish: None to declare.

Conflicts of interest: The authors have no conflicts of interest to report.

Funding/financial support: This study was supported by an internal grant (TEKA/2023).

Unauthenticated | Downloaded 05/06/26 10:44 AM UTC

ACKNOWLEDGMENTS

The authors wish to thank all participants for volunteering in this study.

REFERENCES

1. Faude O, Koch T, Meyer T. Straight sprinting is the most frequent action in goal situations in professional football. J Sports Sci 2012; 30(7): 625–31. https://doi.org/10.1080/02640414.2012.665940
2. Stølen T, Chamari K, Castagna C, Wisløff U. Physiology of soccer: an update. Sports Med 2005; 35(6): 501–36. https://doi.org/10.2165/00007256-200535060-00004
3. Kawamori N, Nosaka K, Newton R. Relationships between ground reaction impulse and sprint acceleration performance in team sport athletes. J Strength Cond Res 2012; 27(3): 568–73. https://doi.org/10.1519/JSC.0b013e318257805a
4. Morin J-B, Bourdin M, Edouard P, Peyrot N, Samozino P, Lacour J-R. Mechanical determinants of 100-m sprint running performance. Eur J Appl Physiol 2012; 112(11): 3921–30. https://doi.org/10.1007/s00421-012-2379-8
5. Dorn T, Schache A, Pandy M. Muscular strategy shift in human running: dependence of running speed on hip and ankle muscle performance. J Exp Biol 2012; 215(11): 1944–56. https://doi.org/10.1242/jeb.064527
6. Pandy M, Lai A, Schache A, Lin Y-C. How muscles maximize performance in accelerated sprinting. Scand J Med Sci Sports 2021; 31(10): 1882–96. https://doi.org/10.1111/sms.14021
7. Morin JB, Gimenez P, Edouard P, Arnal P, Jiménez-Reyes P, Samozino P, et al. Sprint acceleration mechanics: the major role of hamstrings in horizontal force production. Front Physiol 2015; 24(6): 404. https://doi.org/10.3389/fphys.2015.00404
8. Kawama R, Takahashi K, Tozawa H, Obata T, Fujii N, Arai A, et al. Muscle morphological changes and enhanced sprint running performance: a 1-year observational study of well-trained sprinters. Eur J Sport Sci 2024; 24(9): 1228–39. https://doi.org/10.1002/ejsc.12155
9. Miller R, Balshaw TG, Massey GJ, Maeo S, Lanza MB, Johnston M, et al. The muscle morphology of elite sprint running. Med Sci Sports Exerc 2021; 53(4): 804–15. https://doi.org/10.1249/MSS.0000000000002522
10. Takahashi K, Kamibayashi K, Wakahara T. Muscle size of individual hip extensors in sprint runners: its relation to spatiotemporal variables and sprint velocity during maximal velocity sprinting. Plos One 2021; 16(4): e0249670-.
11. Willer J, Allen SJ, Burden RJ, Folland J. How humans run faster: the neuromechanical contributions of functional muscle groups to running at different speeds. Scand J Med Sci Sports 2024; 34(8): e14690. https://doi.org/10.1111/sms.14690
12. Kyröläinen H, Avela J, Komi P. Changes in muscle activity with increasing running speed. J Sports Sci 2005; 23(10): 1101–9. https://doi.org/10.1080/02640410400021575
13. Schache A, Dorn T, Wrigley T, Brown N, Pandy M. Stretch and activation of the human biarticular hamstrings across a range of running speeds. Eur J Appl Physiol 2013; 113(11): 2813–28. https://doi.org/10.1007/s00421-013-2713-9
14. Hegyi A, Gonçalves BAM, Finni T, Cronin NJ. Individual Region- and muscle-specific hamstring activity at different running speeds. Med Sci Sports Exerc 2019; 51(11): 2274–85. https://doi.org/10.1249/MSS.0000000000002060

Unauthenticated | Downloaded 05/06/26 10:44 AM UTC

15. Higashihara A, Nagano Y, Ono T, Fukubayashi T. Differences in activation properties of the hamstring muscles during overground sprinting. Gait Posture 2015; 42(3): 360–4. https://doi.org/10.1016/j.gaitpost.2015.07.002
16. Higashihara A, Nagano Y, Ono T, Fukubayashi T. Differences in hamstring activation characteristics between the acceleration and maximum-speed phases of sprinting. J Sports Sci 2017; 36(12): 1313–8. https://doi.org/10.1080/02640414.2017.1375548
17. Macchi R, Hegyi A, Giroux C, Rabita G, Nordez A, Hollville E, et al. Effects of resistance and speed on electromyographic activity of thigh and gluteal muscles in elite athletes throughout resisted sprint running. Med Sci Sports Exerc 2025; 57(7): 1530–45. https://doi.org/10.1249/MSS.0000000000003689
18. Petrakos G, Morin J-B, Egan B. Resisted sled sprint training to improve sprint performance: a systematic review. Sports Med 2016; 46(3): 381–400. https://doi.org/10.1007/s40279-015-0422-8
19. Lahti J, Huuhka T, Romero V, Bezodis I, Morin J-B, Häkkinen K. Changes in sprint performance and sagittal plane kinematics after heavy resisted sprint training in professional soccer players. PeerJ 2020; 8: e10507. https://doi.org/10.7717/peerj.10507
20. Alcaraz P, Palao J, Elvira J, Linthorne N. Effects of three types of resisted sprint training devices on the kinematics of sprinting at maximum velocity. J Strength Cond Res 2008; 22(3): 890–7. https://doi.org/10.1519/JSC.0b013e31816611ea
21. Cronin J, Hansen K, Kawamori N, McNair P. Effects of weighted vest and sled towing on sprint kinematics. Sports Biomech 2008; 7(2): 160–72. https://doi.org/10.1080/14763140701841381
22. Osterwald KM, Kelly DT, Comyns TM, Catháin CÓ. Resisted sled sprint kinematics: the acute effect of load and sporting population. Sports 2021; 9(10): 137. https://doi.org/10.3390/sports9100137
23. Sugisaki N, Kobayashi K, Yoshimoto T, Mitsukawa N, Tsuchie H, Takai Y, et al. Influence of horizontal resistance loads on spatiotemporal and ground reaction force variables during maximal sprint acceleration. PLoS One 2023; 18(12): e0295758. https://doi.org/10.1371/journal.pone.0295758
24. Cerone GL, Nicola R, Caruso M, Rossanigo R, Cereatti A, Vieira T. Running speed changes the distribution of excitation within the biceps femoris muscle in 80m sprints. Scand J Med Sci Sports 2023; 33(7): 1104–15. https://doi.org/10.1111/sms.14341
25. Upton D. The effect of assisted and resisted sprint training on acceleration and velocity in division IA female soccer athletes. J Strength Cond Res 2011; 25(10): 2645–52. https://doi.org/10.1519/JSC.0b013e318201be16
26. Healy R, Kenny I, Harrison A. Estimating step parameters using photoelectric cells. In: Colloud Floren, Domalain Mathieu, Monnet Tony, editors. 33rd international conference on biomechanics in sports. Poitiers, France; 2015.
27. Hermens HJ, Freriks B, Disselhorst-Klug C, Rau G. Development of recommendations for SEMG sensors and sensor placement procedures. J Electromyogr Kinesiol 2000; 10(5): 361–74. https://doi.org/10.1016/S1050-6411(00)00027-4
28. Woodley SJ, Mercer SR. Hamstring muscles: architecture and innervation. Cells Tissues Organs 2005; 179(3): 125–41. https://doi.org/10.1159/000085004
29. Balius R, Pedret C, Iriarte I, Sáiz R, Cerezal L. Sonographic landmarks in hamstring muscles. Skeletal Radiol 2019; 48(11): 1675–83. https://doi.org/10.1007/s00256-019-03208-x
30. Vieira TM, Botter A. The accurate assessment of muscle excitation requires the detection of multiple surface electromyograms. Exerc Sport Sci Rev 2021; 49(1): 23–34. https://doi.org/10.1249/JES.0000000000000240
31. Vieira TM, Merletti R, Mesin L. Automatic segmentation of surface EMG images: improving the estimation of neuromuscular activity. J Biomech 2010; 43(11): 2149–58. https://doi.org/10.1016/j.jbiomech.2010.03.049

Unauthenticated | Downloaded 05/06/26 10:44 AM UTC

32. Pataky T, Robinson M, Vanrenterghem J. Region-of-interest analyses of onedimensional biomechanical trajectories: bridging 0D and 1D theory, augmenting statistical power. PeerJ 2016; 4: e2652. https://doi.org/10.7717/peerj.2652
33. Pataky T, Vanrenterghem J, Robinson M. The probability of false positives in zero-dimensional analyses of one-dimensional kinematic, force and EMG trajectories. J Biomech 2016; 49(14): 1468–76. https://doi.org/10.1016/j.jbiomech.2016.03.032
34. van den Tillaar R, Gamble P. Comparison of step-by-step kinematics and muscle activation of resisted, assisted, and unloaded 30-m sprints in sprinters. Transl Sports Med 2018; 1(4): 151–9. https://doi.org/10.1002/tsm2.27
35. van den Tillaar R. Effect of active resisted 30 m sprints upon step and joint kinematics and muscle activity in experienced male and female sprinters. J Sports Sci 2021; 39(9): 1060–9. https://doi.org/10.1080/02640414.2020.1856463
36. Spinks C, Murphy A, Spinks W, Lockie R. The effects of resisted sprint training on acceleration performance and kinematics in soccer, rugby union, and Australian football players. J Strength Conditioning Res/Natl Strength & Conditioning Assoc 2007; 21(1): 77–85. https://doi.org/10.1519/R-18145.1
37. Bachero-Mena B, González-Badillo J. Effects of resisted sprint training on acceleration with three different loads accounting for 5, 12.5, and 20% of body mass. J Strength Cond Res 2014; 28(10): 2954–60. https://doi.org/10.1519/JSC.0000000000000492
38. Vieira T, Cerone GL, Botter A, Watanabe K, Vigotsky A. The sensitivity of bipolar electromyograms to muscle excitation scales with the inter-electrode distance. IEEE Trans Neural Syst Rehabil Eng 2023; 31: 4245–55. https://doi.org/10.1109/TNSRE.2023.3325132
39. Sahinis C, Amiridis I, Kannas T, Farina D, Enoka R, Kellis E. Distinct neural drives along the semitendinosus muscle. Med Sci Sports Exerc 2024; 56(12): 2338–48. https://doi.org/10.1249/MSS.0000000000003530

Open Access statement. This is an open-access article distributed under the terms of the Creative Commons Attribution 4.0 International License (https://creativecommons.org/licenses/by/4.0/), which permits unrestricted use, distribution, and reproduction in any medium, provided the original author and source are credited, a link to the CC License is provided, and changes – if any – are indicated. (SID_1)

Unauthenticated | Downloaded 05/06/26 10:44 AM UTC